Hysteresis Circuits and Their Realizations*

A A Shinde,

and

T S Rathore
Dean R&D and Head ET Department
St Francis Institute of Technology, Borivali (W), Mumbai - 400 103

Abstract: *There are four possible types of hysteresis characteristics; two of them are well-documented in the literature while the other two do not appear at all. The circuit realizations of the latter two characteristics are presented in this paper. Range of phase shift provided by each type of hysteresis circuit with respect to the input waveform is given. A typical application involving the use of all the types of hysteresis characteristics is presented. Practical results are included.*

Keywords: Hysteresis characteristics, Schmitt Triggers, NIA, IC, NIC, IA

1. Introduction

The hysteresis characteristics (HCs) can be of inverting or non-inverting type outside the hysteresis loop and the loop itself can be clockwise or anticlockwise. Thus, there can be four possible combinations of the HCs: (i) non-inverting type with anticlockwise hysteresis loop (NIA), (ii) inverting type with clockwise hysteresis loop (IA), (iii) inverting type with anti-clockwise hysteresis loop (NIC), (iv) non-inverting type with clockwise hysteresis loop (IA). They are shown in Fig. 1. Circuits realizing HC (i) and (ii) are popularly known as non-inverting and inverting Schmitt triggers [1]. The realizations of the other two HCs are not covered in well-established books [1]. This papers deals with them. A typical application for realizing an n-phase ($2 \leq n \leq 8$) square wave generator in which all the HCs are required is given. The generator is tested in the laboratory.

From Fig 1, we make the following observations.

1. When the input V_i increases (decreases) from a low (high) value towards a high (low) value NIA and IC change the output state at a threshold voltage V_C ($-V_C$), whereas for NIC and IA the corresponding threshold voltage is $-V_C$ (V_C).
2. NIA–IC and NIC–IA form complementary pairs, i.e., IC (IA) can be obtained by complementing the output of NIA (NIC) and vice versa.

2.1 Circuit realizations of the hysteresis characteristics

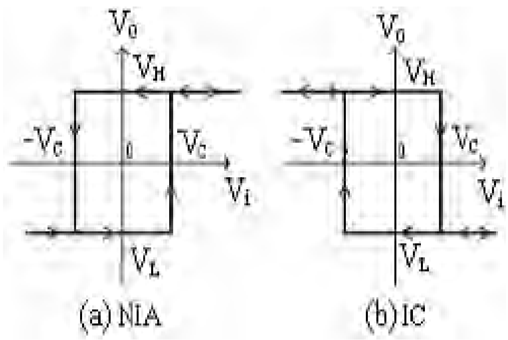

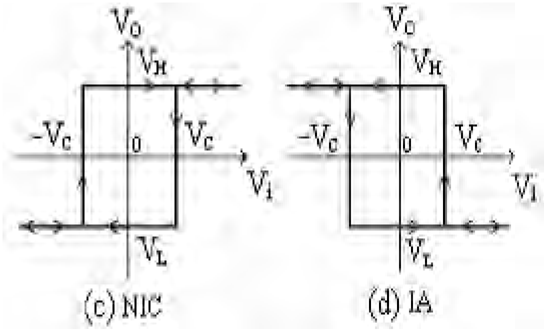

Fig. 1: Hysteresis characteristics

Although an HC can be symmetrical and unsymmetrical, only symmetrical HC will be considered for convenience. Circuits realizing IC and NIA HCs are well-known. Fig 2 shows one possible circuit realization of the NIC HC along with the waveforms. Note that the two threshold voltages V_C and $-V_C$ are required to be applied externally. The IA characteristic of Fig 1(d) is available at the output *Q*.

A simpler circuit using only two Op Amps is shown in Fig 3(a) and the waveforms are shown in Fig 3(b). Non-inverting Schmitt trigger and the comparator C_2 have threshold voltages V_{C1} and V_C, respectively. For proper operation of the circuit,

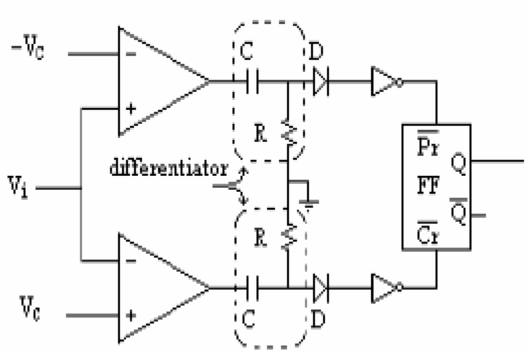

(a)

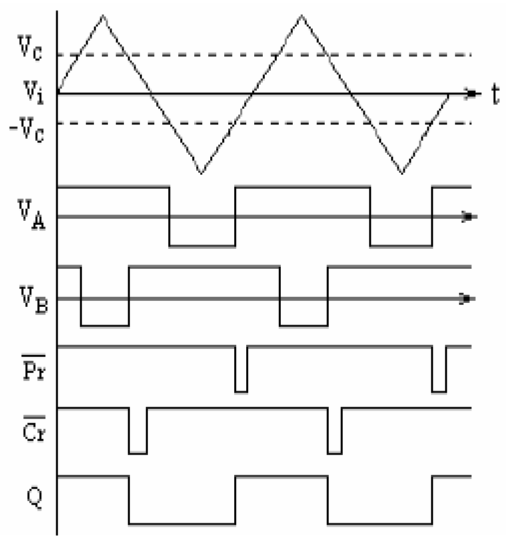

(b)

Fig. 2: (a) The NIC hysteresis circuit, (b) Waveforms

$$V_{C1} \geq V_C \qquad (1)$$

or
$$\frac{R_1}{R_2} V_{sat} \geq \frac{R_4}{R_3 + R_4} V_{sat}$$

where V_{sat} is the output saturation voltage of the non-inverting Schmitt trigger and V_C is the desired threshold voltage of NIC HC.
Hence,

$$R_1(R_3+R_4) \geq R_4R_2 \qquad (2)$$

Note that the desired threshold voltages V_C and $-V_C$ are generated within the circuit itself, reducing the complexity of the circuit as compared to the circuit of Fig 2(a). IA HC can be obtained by interchanging the input terminals of the comparator C_2 in Fig 3(a). Note that the threshold voltage required for the operation of the NIC hysteresis circuit is derived from the output of the NIA HC.

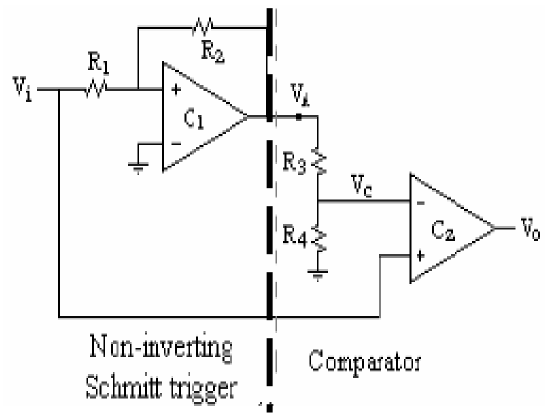

(a)

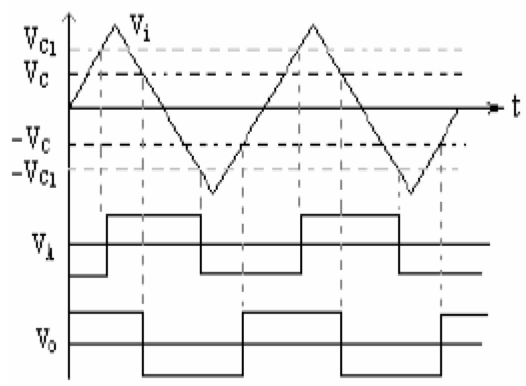

(b)

Fig. 3: (a) Proposed NIC hysteresis circuit, (b) Waveforms

2.2 Input output phase relationship

In Fig 4, a triangular wave is an input to different HCs each with a threshold voltage V_C. Each HC produces a square wave output shifted by an angle φ with respect to the reference triangular wave. Assuming that the triangular wave is perfectly linear, the phase shift φ

Table 1: Input output phase shift relation

Hysteresis characteristic	Phase shift ϕ
NIA	$\frac{\pi}{2}\left(\frac{Vc}{V_P}\right)$
IA	$\frac{\pi}{2}\left(2-\frac{Vc}{V_P}\right)$
IC	$\frac{\pi}{2}\left(2+\frac{Vc}{V_P}\right)$
NIC	$\frac{\pi}{2}\left(4-\frac{Vc}{V_P}\right)$

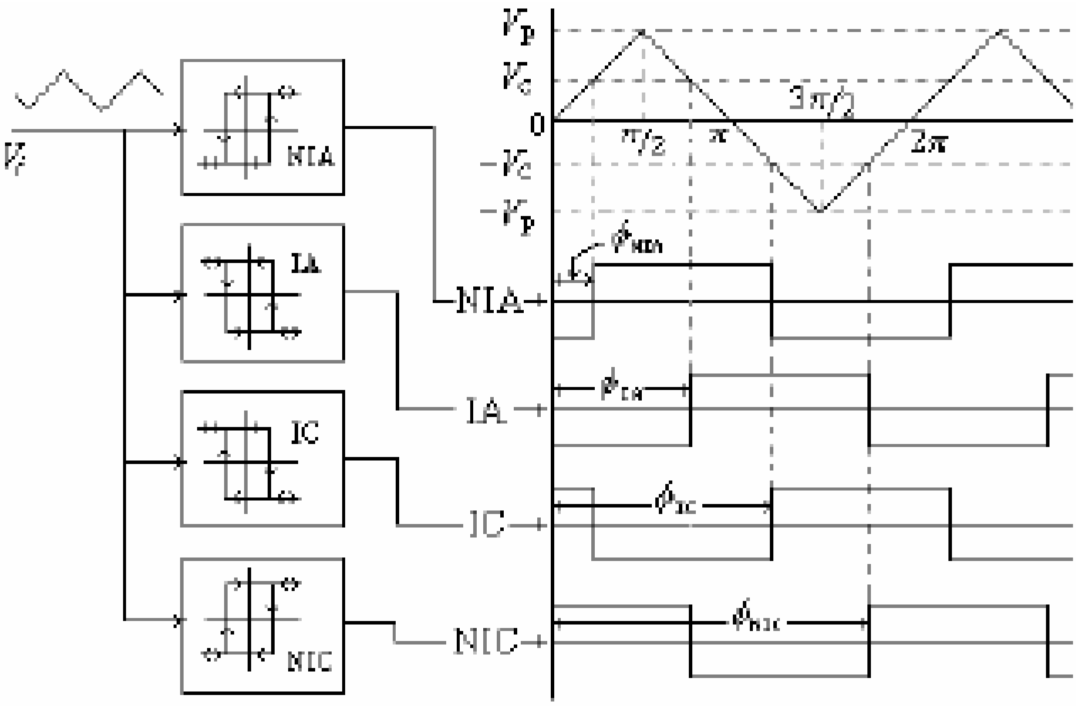

Fig. 4: Input and output waveforms of different hysteresis circuits

produced by each HC is given in Table 1. Since $0 \leq V_C \leq Vp$, it can be seen from the φ -relation in Table 1 that each HC produces φ which covers a distinct quadrant as shown in Fig

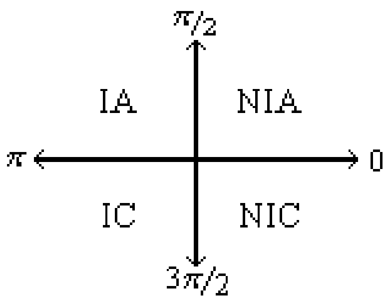

Fig. 5: Phase distribution

2.3 Complementary Property

Just as inverting and non-inverting amplifiers can be obtained by interchanging input and ground terminals [2], NIC (NIA), so also HC can be obtained from its complementary circuit IA (IC) by interchanging the input and ground terminals. This is shown in Fig 6. The operating condition, i.e., $V_{C1} \geq V_C$ remains the same for both NIC and IA HCs.

3. Test results

The operation of the circuit of Fig 3(a) is verified both on the circuit simulator (Multisim), and on a bread

Fig. 6: Conversion diagram for hysteresis circuits

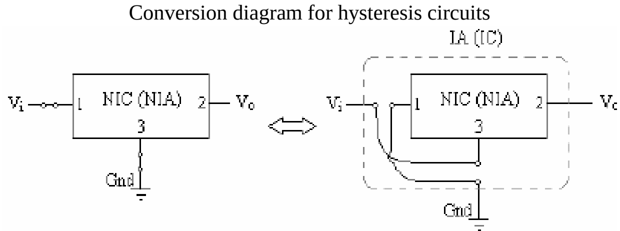

board. The circuit exhibited the hysteresiso characteristic as expected when $V_{C1} < V_C$. However, when the input V_i is such that $V_{C1} \leq Vi \leq V_C$, the threshold voltage for comparator C_2 inverts and hence the output appears as inverted form of the desired output. To achieve better accuracy, the threshold voltages V_C and V_{C1} must be stable and accurate.

4. Application

One typical application that involves the use of all the hysteresis circuits is an *n*-phase square wave generator [3]. The block diagram of the generator is shown in Fig 7. The circuit shown in the dashed box is a conventional function generator consisting of an inverting (Miller) integrator and a non-inverting Schmitt trigger [1] whose threshold voltage is V_p = the peak value of the triangular wave. HB_i has threshold voltage V_{Ci}. The square wave output of HB_1 is assigned as the reference phase which itself is displaced by an angle 90° with respect to the input triangle wave.

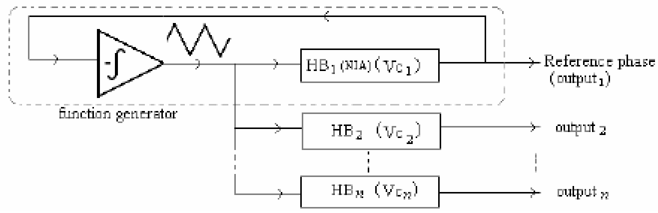

Fig. 7: Block diagram of an *n*-phase square wave generator

Phase angles of all the phases in an *n*-phase system are measured with respect to the reference phase. Hence, the phase distribution plane for this application will be that of Fig 5 rotated by 90° in clockwise direction, and is as shown in Fig. 8. The corresponding phase shift is given in Table 2.

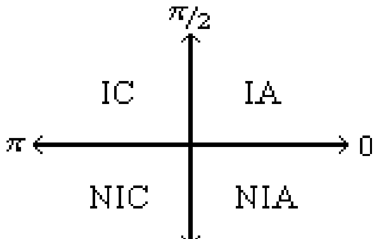

Fig. 8: Phase distribution for *n*-phase generation system

Table 2: Phase shift for the hysteresis characteristics used in n-phase generation system

Hysteresis characteristic	Phase shift φ
IA	$\frac{\pi}{2}\left(1-\frac{Vc}{V_P}\right)$
IC	$\frac{\pi}{2}\left(1+\frac{Vc}{V_P}\right)$
NIC	$\frac{\pi}{2}\left(3-\frac{Vc}{V_P}\right)$
NIA	$\frac{\pi}{2}\left(3+\frac{Vc}{V_P}\right)$

Since, phase φ_i for the i^{th} phase of n-phase system is

$$\phi_i = \left(\frac{2\pi}{n}\right)(i-1),\ 2 \le i \le n, \qquad (3)$$

choose the appropriate hysteresis circuit from Fig 8 and then choose the appropriate V_C from the corresponding relations given in Table 2. From Fig 8, it is seen that two adjacent quadrants share a common phase of 0, $\pi/2$, π and $3\pi/2$. Hence either circuit belonging to the adjacent quadrant can be used. For example, for a phase shift of $\pi/2$, one may choose IA or IC. However for HB_1 the NIA is already chosen because of the inverting integrator. A system for $2 \le n \le 8$ is designed, for which Table 3 shows allocation of various phases where X indicates a valid phase output at the corresponding hysteresis block. For example, when $n = 5$, hysteresis blocks HB_1, HB_2, HB_4, HB_6 and HB_8 will provide valid phase outputs and the phase sequence will be Phase1, Phase2, Phase3, Phase4 and Phase5. The outputs of the remaining hysteresis blocks will be ignored.

Table 3: Phase allocation

Hysterises block	Type of hysteresis circuit	Number of phases, n						
		8	7	6	5	4	3	2
HB_1	NIA	X	X	X	X	X	X	X
HB_2	IA	X	X	X	X			
HB_3	IC	X	X			X		
HB_4	IC	X	X	X	X		X	
HB_5	IC	X		X		X		X
HB_6	NIC	X	X	X	X		X	
HB_7	NIC	X	X			X		
HB_8	NIA	X	X	X	X			

The circuit realization of the n phase ($2 \le n \le 8$) symmetrical system is shown in Fig 9. Here each hysteresis block has a provision for adjusting its reference voltage, depending on the value of n, through programmable resistors. For better accuracy, the resistor values are chosen such that they are much smaller (larger) than the off (on) resistances of the switches.

Since NIA hysteresis circuit is already used to generate the reference phase, it is also used to generate the required threshold voltages for the NIC of HB_6, HB_7 and the IA of HB_2 to reduce one opamp in each of these hysteresis circuits. As V_p is always greater than the threshold voltage required for any other hysteresis circuit, the condition $V_{C1} \ge V_C$ is automatically satisfied.

The circuit uses in all 9 opamps. In general, for n phase system, $n + 1$ opamps will be required. The integrator output peak V_p is precisely adjusted to the zener reference voltage at the output of the hysteresis block HB_1. Programmable resistors are used to change the threshold voltages of the hysteresis blocks as per the requirement. The frequency can be adjusted (programmed) by the variable potentiometer (digitally controlled) R.

Table 4 shows the status of switches required for generating different number of phases in the system.

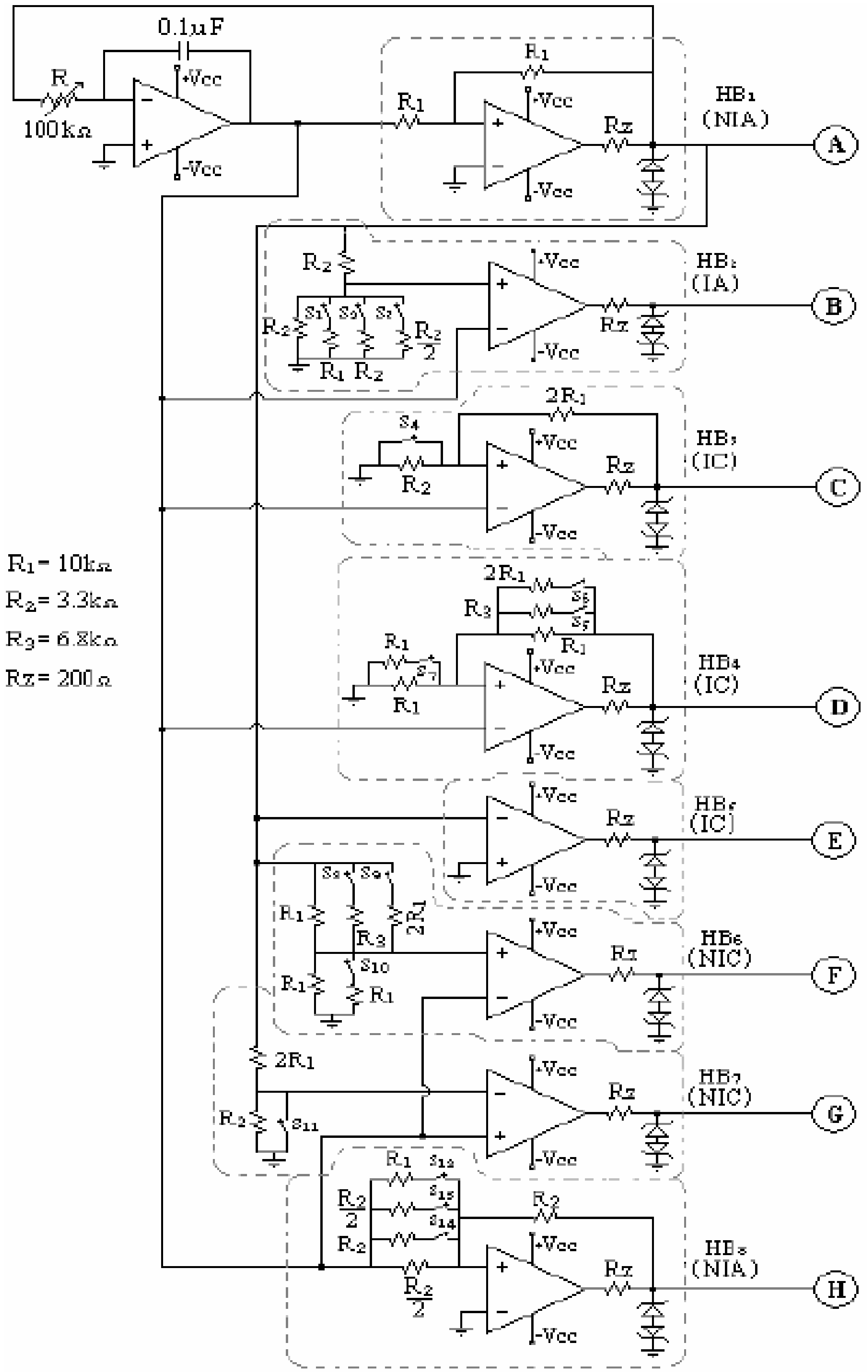

Fig. 9: Programmable *n* phase ($2 \le n \le 8$) symmetrical phase system

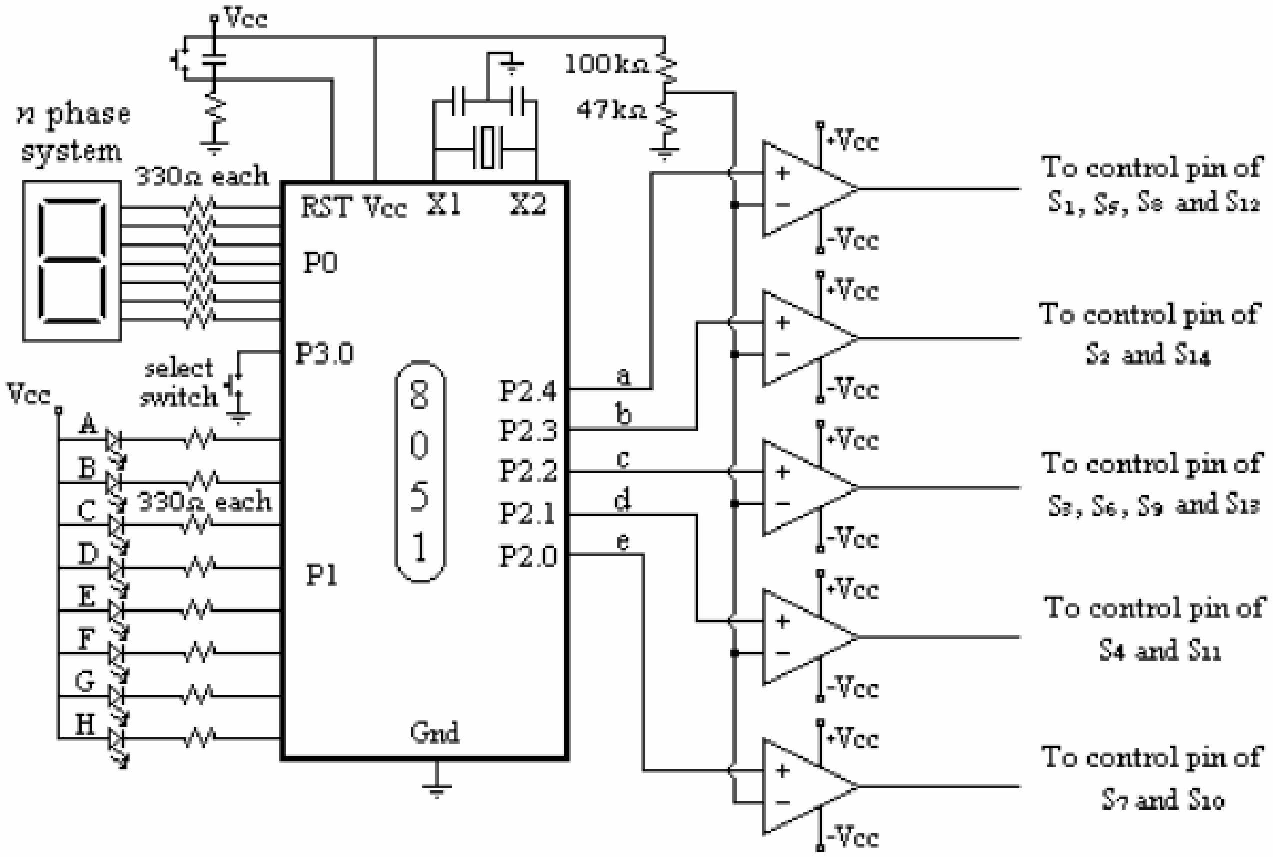

Fig. 10: Control circuit for the programmable multiphase generator

Table 4: Switch status for the programmable multiphase generator

n	S_1, S_5, S_8 and S_{12}	S_2 and S_{14}	S_3, S_6, S_9 and S_{13}	S_4 and S_{11}	S_7 and S_{10}
8, 4, 2	Off	Off	Off	On	Off
7	On	Off	Off	Off	Off
6, 3	Off	On	Off	Off	On
5	Off	On	On	Off	Off

A control circuit used for the system of Fig. 9 is shown in Fig. 10.

A micro-controller 8051 [4] is used to control the operation of various switches. Desired *n*-phase system is selected using a push button switch connected to one of the port pins of the micro-controller. Seven- segment LED indicates the present selection. Eight LEDs are connected to indicate which output is valid for a particular value of *n*.

As the switches are to operate to produce both the positive and negative threshold voltages, TTL level control signals are converted into bipolar signals using comparators. Software flow for the program is shown in Fig 11. The flow chart shows various processes

carried out by the micro-controller to perform various actions. Software is written in 8051 assembly level language [4]. Look up tables are stored in memory to output appropriate logic on the control lines and to switch on proper LED at the valid phase output.

Though the digitally implemented multiphase square wave generator [5] is faster and cheaper than the analog implementation discussed in the report, the latter has the following advantages.

- Analog implementation has a wide operating frequency range, whereas the operating frequency range of the digital implementation is limited to maximum number of delay stages used.
- Analog implementation has higher output voltage levels than the digital implementation.

- The digital implementation needs a specific amount of time to estimate the period of reference clock and make a decision for selection
of suitable delay range [5]. There is no latency involved in the given analog implementation.

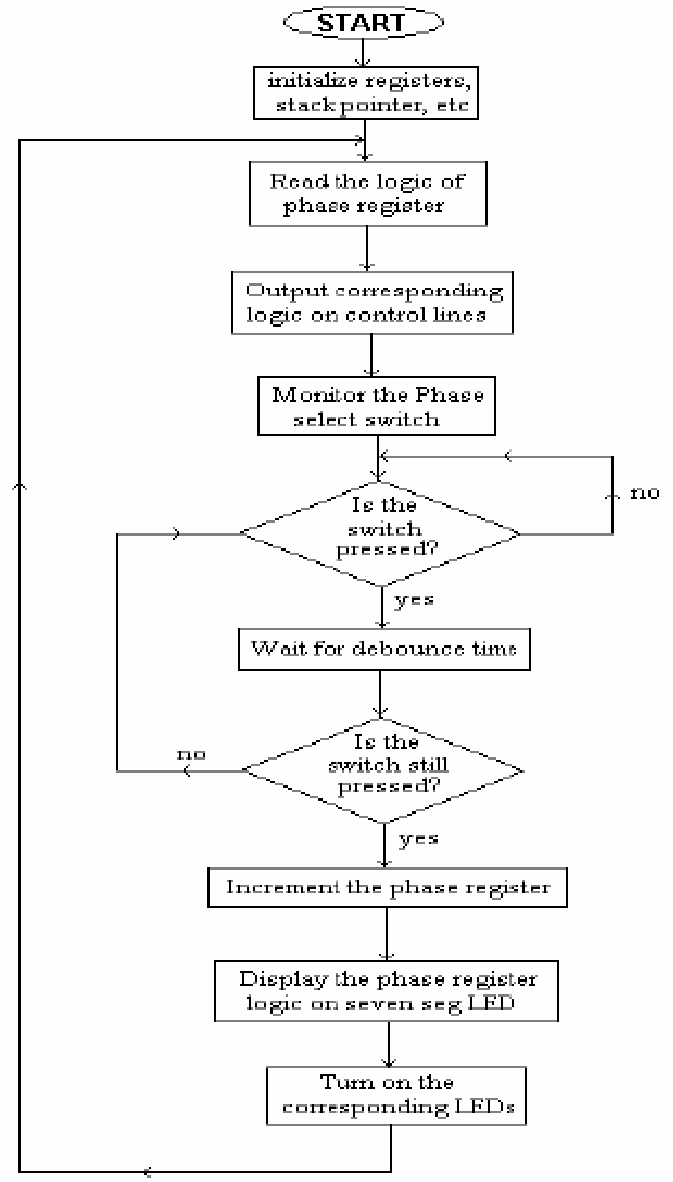

Fig. 11: The Flow diagram

5. Experimental Results

The *n*-phase square wave generator has been tested for its operation. Measurements with digital supply of +5 V and analog supply of $\pm$8 V were taken on a CRO. Resistances of $\pm$10% tolerance were used. For quad Op Amp TL084, the maximum phase error observed was -4° for frequencies up to 8 kHz. The phase error increases with the further increase in operating frequency. Fig 12 shows the plot of phase error v/s frequency for n = 8.

6. Conclusions

A simple circuit for a non-inverting clockwise hysteresis characteristic (NIC) has been proposed. IA

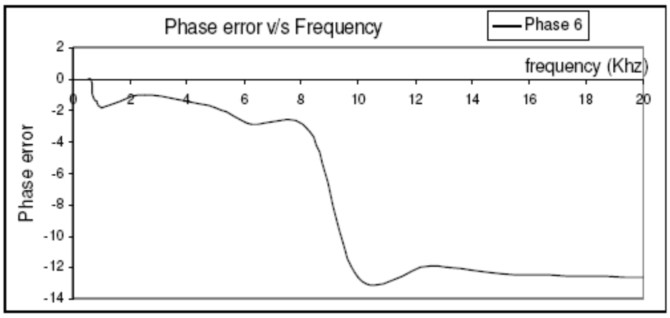

Fig. 12: The plot of phase error v/s frequency

characteristics can be realized by taking the complementary output of NIC. Range of phase shift for each type of hysteresis characteristics has been derived. Each one covers a special quadrant. A typical application (*n*-phase clock generator) in which all the frequencies or channels are needed has been presented. The design of such a circuit has been developed. The generator has been fabricated for $2 \le n \le 8$ and found to work satisfactorily.

References

[1] James M Fiore, *Opamps and Linear Integrated Circuits, Delmar*, Thomson learning, 2001

[2] T S Rathore and B M Singhi, *Network Transformations,* IEEE Trans Circuits Syst, 27, 57-59, Jan 1980

[3] R Rabinovici, Multihysteresis block as a polyphase square wave oscillator, IEEE Trans Industrial Electronics, IE-44, 427-428, June 1997

[4] Kenneth J Ayala, *The 8051 Microcontroller* Architecture, Programming and Applications, Penram International, Second Edition, 1996

[5] Ching-Che Chung and Chen-Yi Lee, *A New DLL-Based Approach for All-Digital Multiphase Clock Generation,* IEEE J of Solid-State Circuits, 39, Mar 2004

AUTHORS PROFILE

T S Rathore was born in Jhabua (M P, India) on Oct. 29, 1943. He received the B Sc (Electrical Engineering), M E (Applied Electronics & Servomechanisms), and Ph D (by research on Passive and Active Circuits) degrees in Electrical Engineering from Indore University, Indore, India in 1965, 1970 and 1975, respectively.

He served SGSITS, Indore from 1965 to 1978 before joining the EE Department of IIT Bombay from where he retired as a Professor on superannuation in June 2006. Currently, from July 2006, he is the Dean (R&D) and Head of Electronics & Telecommunication Department at St. Francis Institute of Technology, Borivali.

He was a post-doctoral fellow (1983-85) at the Concordia University, Montreal, Canada and a visiting researcher at the University of South Australia, Adelaide (March-June 1993). He was an ISTE visiting professor (2005-2007). He has published and presented over 205 research papers in various national/international journals and conferences. He has authored the book Digital Measurement Techniques, New Delhi: Narosa Publishing House, 1996 and Alpha Science International Pvt. Ltd., U K, 2003 and translated in Russian language in 2004. He was the Guest Editor of the special issue of Journal of IE on Instrumentation Electronics (1992). He is a member on the editorial boards of ISTE National Journal of Technical Education and IETE Journal of Education. He has witnessed, organized and chaired many national/international conferences and in some he was also the Chief Editor of the proceedings.

His areas of teaching and research interest are Analysis and Synthesis of Networks, Electronic Circuit Design, Switched-Capacitor Filters, Electronic-Aided Instrumentation, Hartley Transform, Signal Processing, Fault Diagnosis and Knowledge-Based Systems.

Prof. Rathore is a Senior Member of IEEE (USA), Fellow of IETE (India), Fellow of IE (India), Member of ISTE (India), Member of Instrument Society of India, Member of Computer Society of India. He has been listed in Asia's Who's Who of Men and Women of achievement (1991). He has played a very active role as

Fellow of IETE and has served its Mumbai Centre as Volunteer member (1997-98), Co-opted member (1998-99), Secretary (1999-2001), Chairman (2001-02), Vice Chairman (2003-06) and Chairman (2006-08).

He has received IETE M N Saha Memorial Award (1995), IEEE Silver Jubilee Medal (2001), ISTE U P Government National Award (2002), ISTE Maharashtra State National Award (2003), IETE Prof S V C Aiya Memorial Award (2004), IETE BR Batra Memorial Award (2005), IETE Prof K Sreenivasan Memorial Award (2005). IETE K S Krishnan Memorial Award (2009), IETE Hari Ramji Toshniwal Gold Medal Award (2010), and IETE best paper award published in IETE J of Education (2011).